
Smiles2Dock: a large-scale dataset for ML-based docking score prediction using AlphaFold structures

Anonymous Author(s)

Affiliation

Address

email

Abstract

1 Docking is a crucial component in drug discovery aimed at predicting the binding
2 conformation and affinity between small molecules and target proteins. ML-based
3 docking has recently emerged as a prominent approach, outpacing traditional
4 methods like DOCK and AutoDock Vina in handling the growing scale and com-
5 plexity of molecular libraries. However, the availability of comprehensive and
6 user-friendly datasets for training and benchmarking ML-based docking algorithms
7 remains limited. Moreover, existing datasets rely on proteins with experimentally
8 determined structures and known ligand binding pockets, making them unusable
9 for the growing number of proteins with only predicted structures. We introduce
10 Smiles2Dock, an open large-scale dataset for molecular docking that addresses this
11 gap. We created a framework combining P2Rank for binding pocket prediction
12 and AutoDock Vina for docking, enabling us to dock 1.7 million ligands from the
13 ChEMBL database against 11 genetically validated proteins from AlphaFold, re-
14 sulting in over 17 million protein-ligand binding scores. Since AlphaFold-predicted
15 structures do not include known ligand binding sites, our use of P2Rank allows
16 docking to be performed without any experimental structure information, a first
17 at this scale. The dataset encompasses a diverse set of biologically relevant com-
18 pounds and enables researchers to benchmark all major approaches for ML-based
19 docking such as Graph, Transformer, and CNN-based methods. We also introduce
20 a novel Transformer-based architecture for docking score prediction and set it as
21 an initial benchmark for our dataset.

22 Introduction

23 Molecular docking is a computational technique used to predict how a small molecule binds to a
24 protein target [30]. By estimating the ligand's position and orientation within the binding site, docking
25 helps assess how well a compound might interact with and modulate the protein's function [31].
26 Traditional molecular docking methods use scoring functions designed to estimate how strong the
27 interaction is between a protein and a ligand based on their 3D arrangement. These scoring functions
28 are based on physical and chemical principles that estimate binding strength from a predicted 3D
29 pose of the ligand in the protein. On the other hand, docking score predictors are Machine Learning
30 (ML) models that learn to predict docking scores directly from molecular graphs or sequences.

31 Traditional docking

32 Docking is widely used in drug discovery to screen large libraries of compounds and prioritize those
33 most likely to bind effectively, reducing the need for costly synthesis and experimental testing [14, 38].
34 Docking algorithms output binding scores and poses, which estimate binding affinity and suggest
35 how a ligand fits into the protein's active site. These predictions guide the selection of promising

36 compounds for further development. Effective docking results forecast where and how well a ligand
37 binds and provide insights into the nature of the binding affinity and specificity.[30].

38 As the scale of molecular libraries expands dramatically in drug discovery, the need for faster
39 and more efficient docking tools has become key. Traditional scoring functions such as DOCK,
40 which relies on geometric matching algorithms to fit ligands into protein binding sites; AutoDock
41 Vina, which uses gradient-based optimization to predict binding poses; and Glide, which performs
42 systematic searches across ligand conformations, orientations, and positions, have proven too slow
43 to handle modern large-scale libraries [6, 43, 11]. In response, researchers are turning to machine
44 learning (ML) docking score predictors - models trained to replicate docking scores generated by
45 programs like AutoDock Vina. When deployed on GPUs, these models can predict binding outcomes
46 significantly faster than traditional methods, achieving speedups of 10 to 100 times [7].

47 **ML-based docking**

48 Machine learning-based docking algorithms can be broadly divided into two categories: (1) docking
49 score predictors, which directly estimate the binding affinity or docking score between a protein
50 and a ligand, and (2) end-to-end docking methods, which predict the score as well as binding poses
51 and affinities from structural or sequence-based inputs. Each branch leverages different model
52 architectures to address the complexity of molecular interactions. Several ML approaches have
53 been tried. The most prominent one is Graph Neural Networks (GNNs), which directly model the
54 molecular structure of proteins and ligands as graphs where atoms are nodes and bonds are edges
55 [20, 44, 17].

56 An extension of Graph Neural Networks (GNNs) is Graph Convolutional Networks (GCNs), which
57 apply convolutional operations to graph-structured data, allowing the model to capture the topological
58 features of molecules and their potential interactions with proteins [41] and predict their docking
59 score. Similarly, Transformer-based architectures, originally designed for natural language processing,
60 have been adapted for molecular data by treating atoms or fragments as sequence elements. These
61 models, which can be pretrained on large corpora of SMILES strings, effectively capture long-range
62 dependencies within molecules and across molecular complexes, ultimately representing proteins and
63 ligands as embedding matrices or vectors [16, 15, 4].

64 Computer vision-based approaches, such as 3D Convolutional Neural Networks (3D CNNs), extend
65 the concept of convolution into three dimensions, making them well-suited for modeling the spatial
66 structure of molecules and the 3D configuration of protein-ligand interactions [46, 19] and are
67 typically used for predicting binding scores rather than binding poses. However, GNINA integrates
68 deep learning with traditional docking pipelines to predict both poses and affinities, making it an
69 example of an end-to-end docking model [29].

70 Finally, reinforcement learning has been explored as an end-to-end solution, particularly through the
71 asynchronous advantage actor-critic (A3C) framework. These methods treat docking as a sequential
72 decision-making process, with actor models guiding search strategies and critic models evaluating
73 them, allowing direct prediction of binding poses and improving docking performance [3, 1].

74 **Datasets for molecular docking**

75 The downside of ML-based methods is the amount of data required for training. To solve this, several
76 groups have attempted to build open-source docking datasets by using docking software predictions
77 as inputs for ML models [5, 12, 27, 42]. However, available large-scale docking datasets have several
78 limitations, notably scale, ease of use and lack of generalizability. Some focused on a specific set of
79 proteins linked to a certain disease (e.g. SARS-COV2 proteome), greatly reducing generalization
80 capabilities for ML models trained on those. Others used a number of ligands not in the scale of
81 modern compound libraries, which often have millions of data points, and did not use well-known
82 extensively tested chemical libraries.

83 **Lack of experimental protein structures**

84 Reliable docking requires accurate 3D structures of proteins, especially their binding sites. These are
85 typically obtained through experimental techniques like X-ray crystallography or cryo-EM, which
86 are slow, expensive, and often infeasible, particularly for membrane proteins or unstable targets. As a
87 result, only about 17% of the human proteome has experimentally resolved structures [32]. Existing

88 ML docking datasets like DOCKSTRING and DUD-E rely on these experimentally determined
 89 proteins and annotated binding sites, making them unusable for the majority of proteins with only
 90 predicted structures. Smiles2Dock is the first large-scale dataset to enable docking on proteins without
 91 any experimental structural data. We use AlphaFold-predicted 3D structures, which cover nearly the
 92 entire human proteome, and apply P2Rank to predict binding pockets directly from the structure.
 93 This lets us perform docking using AutoDock Vina on 11 genetically validated AlphaFold targets and
 94 1.7 million ChEMBL ligands, resulting in over 17 million docking scores. All binding site predictions
 95 are released for reuse. Ligands are represented using SMILES strings, supporting Transformer-based,
 96 graph-based, and 3D computer vision models. The full dataset is hosted on Hugging Face, and can be
 97 loaded with just two lines of Python code [25, 23].

98 Results

99 Correlation and variability of docking scores

100 We computed the Pearson correlation coefficient between docking scores (Figure 1). A subset of
 101 proteins including *slc30a8*, *dpp9*, and *ifih1* formed a highly correlated cluster ($r > 0.8$), suggesting
 102 shared ligand binding preferences and possibly similar pocket chemotypes. Proteins such as *adcy5* and
 103 *cfrh5* exhibited weak correlations ($r < 0.3$) with most others, reflecting distinct binding environments
 104 or limited cross-reactivity with the ligand set. Boxplot analysis (Figure 2) revealed most proteins
 105 showed compact interquartile ranges and moderate outlier counts, consistent with well-behaved
 106 docking score distributions. Proteins such as *cfrh5* demonstrated particularly tight distributions,
 107 whereas *dpp9* and *nrlp3* showed larger score spreads and several high-affinity outliers (scores < -12
 108 kcal/mol).

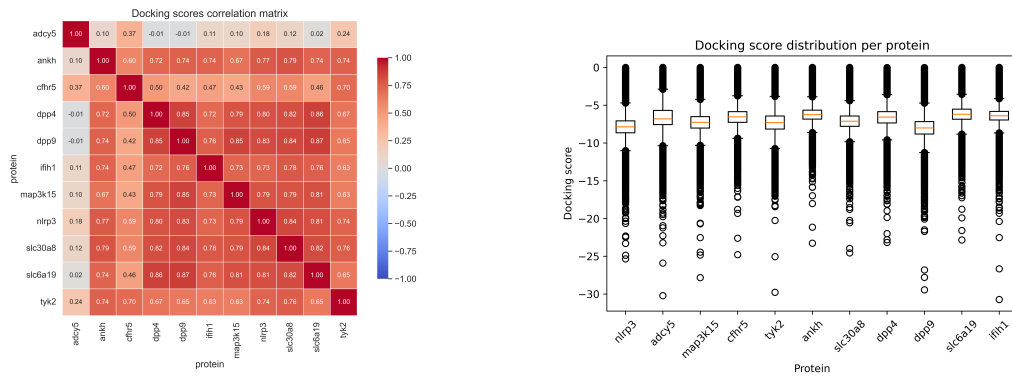


Figure 1: Correlations of docking scores per protein.

Figure 2: Boxplots of docking scores per protein.

109 Distribution of docking scores

110 Our initial hypothesis after looking at Figure 3 was that scores for each protein were normally
 111 distributed. We performed Shapiro-Wilk tests to test for normality of scores distribution for each
 112 protein but all p-values were below the 0.05 significance threshold. [35]. We discovered, by computing
 113 a Q-Q plot (Figure 4), that the distribution was heavily right-skewed, which was also confirmed by
 114 computing the skewness of the distribution of scores for each protein, with values ranging from 5
 115 to 20 (heavily right skewed) [28]. Finally, we tested for right-skewed distributions by performing a
 116 Kolmogorov-Smirnov test for goodness of fit using Log-Normal and Weibull distributions but again
 117 found p-values for all proteins below the significance threshold required [2].

118 Metrics for evaluating models

119 To evaluate model performance in docking score prediction, we use ranking-based metrics that focus
 120 on the relative ordering of compounds rather than their absolute scores. This aligns with the practical

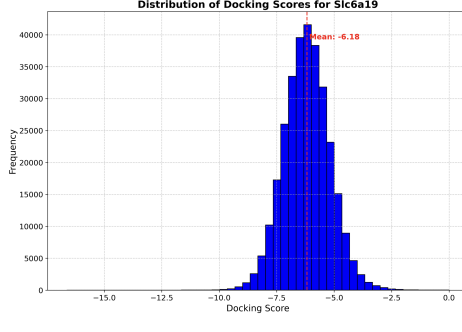


Figure 3: Scores distribution for protein Slc6a19.

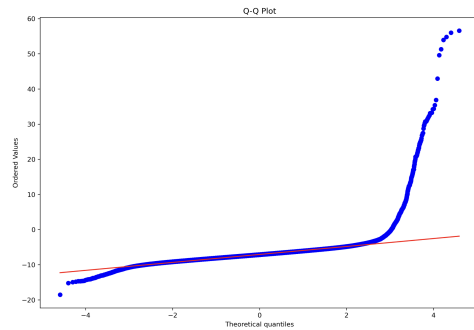


Figure 4: QQ plot for protein Slc6a19.

121 goal in drug discovery: prioritizing a small number of compounds for experimental validation, where
 122 identifying the top candidates is more important than accurately modeling the full score distribution.
 123 Spearman correlation is well-suited here, as it quantifies the agreement between predicted and true
 124 rankings across the dataset [45]. The Spearman rank correlation coefficient (ρ) is a non-parametric
 125 measure of statistical dependence that captures how well the relationship between two variables
 126 follows a monotonic trend. Given predicted and true docking score vectors \hat{y} and y , we denote their
 127 ranks by:

$$\text{rank}(\hat{y}_i) = R_i, \quad \text{rank}(y_i) = S_i.$$

128 Then the Spearman correlation is given by:

$$\rho = 1 - \frac{\sum_{i=1}^n (R_i - S_i)^2}{n(n^2 - 1)}.$$

129 The top- k overlap measures how well the model identifies the most promising compounds. This
 130 metric ranges from 0 to 1. A value of 1 indicates perfect agreement between the predicted and true
 131 top- k ligands, while 0 indicates no overlap. Define T_k , the set of indices corresponding to the top- k
 132 ligands based on the true scores, and \hat{T}_k , the set of indices corresponding to the top- k ligands based
 133 on the predicted scores. Then the top- k overlap is defined as:

$$\text{Top-}k \text{ overlap} = \frac{|T_k \cap \hat{T}_k|}{k}$$

134 Hybrid model results

135 Table 1 presents Spearman correlation and top- k overlap metrics for various model configurations,
 136 varying protein model (PM), ligand model (LM), hidden layer (HL) sizes, and dropout rates. The
 137 best overall performance is achieved by the model with PM=128, LM=256, HL=64, and dropout 0.1,
 138 showing the highest Spearman correlation of 0.76 at the top 50% and maintaining good correlation
 139 (0.24) even at the top 1%. This suggests a good balance between model capacity and regularization.
 140 Larger models with higher dropout (e.g., PM=256, LM=512) show lower Spearman correlations and
 141 top- k overlaps, which may indicate over-regularization or difficulty training such large architectures
 142 on the dataset. Smaller models (e.g., PM=64, LM=64) perform moderately well but generally fall
 143 short of the best configuration. As expected, top- k overlap decreases with stricter cutoffs (from top
 144 50% to top 1%), reflecting the increasing challenge of identifying the very best candidates. Overall,
 145 moderate-sized models with moderate dropout provide the most consistent and accurate ranking
 146 performance.

147 Limitations

148 **P2Rank as a probabilistic framework for binding site prediction:** P2Rank uses an ML-based
 149 algorithm to predict the binding sites of each protein along with an associated probability. We used
 150 an arbitrary threshold to define what counted as a "valid" binding site. In the case where we had
 151 multiple binding sites above our 50% threshold, we only used the one with the highest probability.

PM size	LM size	HL size	Dropout	Top 50%	Top 25 %	Top 10 %	Top 1 %
128	256	64	0.1	0.76 / 0.45	0.64 / 0.33	0.51 / 0.16	0.24 / 0.02
256	512	128	0.2	0.63 / 0.05	0.34 / 0.18	0.18 / 0.16	0.10 / 0.05
64	64	128	0.2	0.73 / 0.38	0.55 / 0.34	0.41 / 0.20	0.21 / 0.06
128	256	128	0.2	0.44 / -0.22	0.15 / 0.06	0.04 / 0.16	0.05 / 0.07
128	128	256	0.1	0.62 / 0.03	0.32 / 0.16	0.16 / 0.16	0.10 / 0.05
256	512	64	0.2	0.67 / 0.15	0.43 / 0.20	0.28 / 0.15	0.16 / 0.04
256	256	256	0.2	0.64 / 0.08	0.37 / 0.18	0.21 / 0.16	0.13 / 0.06
64	128	64	0.2	0.56 / -0.07	0.25 / 0.11	0.10 / 0.15	0.07 / 0.04

Table 1: Spearman correlation (left) and top-k overlap (right) for different percentiles of top scores (PM = Protein model, LM = Ligand model, HL = Hidden layer).

152 **Conformational space exploration:** We used an exhaustiveness parameter of 8 and tried 5 different
 153 poses, the default values for Vina which are known in other studies for balancing accuracy and
 154 computational resource use. Increasing those further would not have been feasible but it could be
 155 beneficial for future studies to do a more thorough search. We also limited ourselves to one binding
 156 site per protein, both for computational resources and also to standardize the prediction task for ML
 157 researchers. However, it could be interesting to look at algorithms that can work on multiple binding
 158 sites at the same time.

159 Methods

160 **AlphaFold:** AlphaFold is an ML model developed by DeepMind designed to predict protein structures
 161 and solve the protein structure prediction problem, which involves determining a protein’s three-
 162 dimensional shape from its amino acid sequence [21]. Its predictions have been extensively validated,
 163 with a reported root-mean-square deviation (RMSD) of around 1.5 Ångströms for many proteins,
 164 comparable to experimental methods like X-ray crystallography and cryo-electron microscopy, while
 165 being significantly cheaper and faster.

166 **ChEMBL:** ChEMBL is a bioactivity database maintained by the European Bioinformatics Institute,
 167 containing detailed information on the biological activity of 2.3M small molecules [13]. It is widely
 168 used for drug discovery and development, offering data on compound properties, target interactions,
 169 and pharmacological profiles.

170 **P2Rank:** P2Rank is an ML model for predicting ligand-binding sites on proteins by analyzing surface
 171 patches based on features like hydrophobicity, electrostatic potential, and geometric arrangement of
 172 atoms [24]. Each protein surface is segmented into patches, with the random forest model assessing
 173 the likelihood of each patch being a binding site based on the extracted features. An example of the
 174 binding pocket predicted by P2Rank for protein adcy5 can be seen on figure 6.

175 **AutoDock Vina:** AutoDock Vina is a popular molecular docking package widely used in computa-
 176 tional chemistry for predicting the interactions between a protein and a ligand. It uses a scoring
 177 function to estimate the strength and stability of a ligand when docked into a protein’s binding site.

178 Dataset preparation

179 In our study, we developed a dataset of molecular docking scores using a comprehensive framework
 180 to ensure precise predictions of protein-ligand interactions, which can be seen in Figure 5.

181 Ligand preparation

182 For ligands, we downloaded the ChEMBL database and used the 2.3M SMILES strings available.
 183 Out of this set, around 20% could not be processed by AutodockVina because of errors, either
 184 when converting SMILES strings to .sdf files using RDKit or due to atom types incompatible with
 185 Autodock. This left us with a set of approximately 1.7M ligands to dock. Then the ligands were
 186 deprotonated at ph 7.4 with OpenBabel. Finally, a 3D conformation was generated using RDKit and

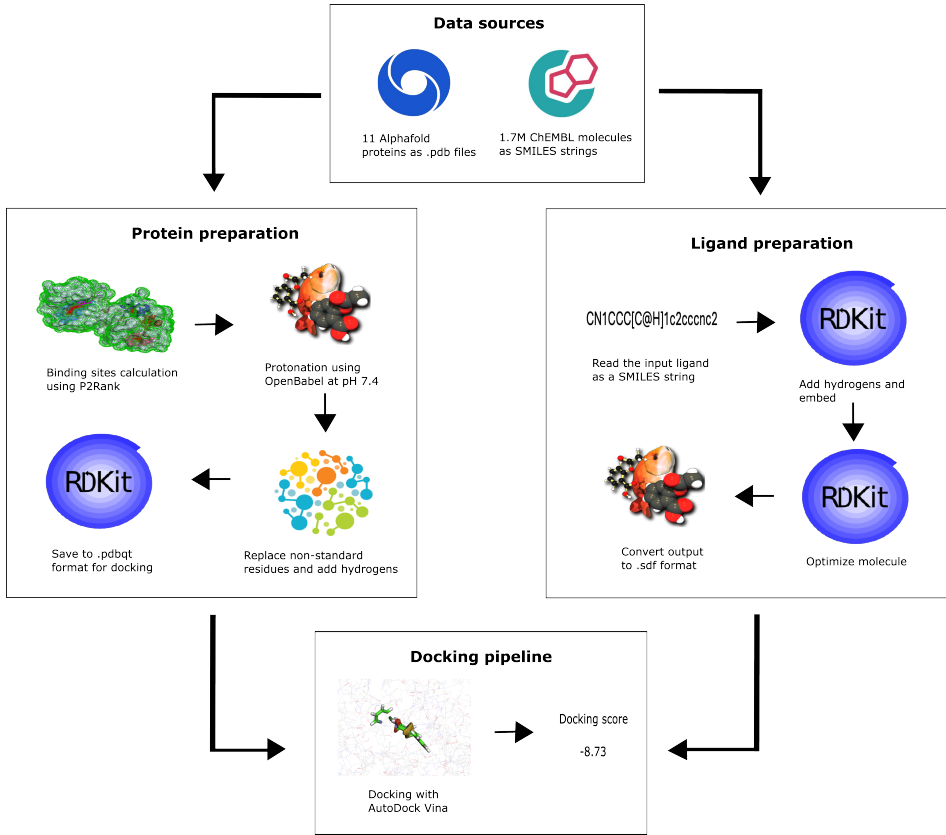


Figure 5: Diagram of the methodology followed for this project.

187 the ETKG algorithm, which we further refined using the classical force field MMFF94. Finally, we
 188 outputted a PDBQT file for each ligand, which is the file format required by AutoDock Vina.

189 **Protein preparation**

190 For proteins, we started with a set of 30 proteins from the AlphaFold database based on their
 191 identification as therapeutic targets in previous genetic association studies [39, 37, 40, 8]. These are
 192 proteins where natural human mutations (identified through GWAS) have been linked to protection
 193 from or risk of disease. This selection strategy is based on work by Plenge et al. [34], which showed
 194 that using human genetics can improve the chances of translating a target into a successful therapy. For
 195 each protein, we looked at their average pLDDT scores and confidence levels from AlphaFold models
 196 and only selected proteins which had an average pLDDT score of High. Finally, we used P2Rank to
 197 predict each protein's binding sites and only kept proteins for which we had at least one site with a
 198 probability above 50%.

199 Protein structures were preprocessed using a custom pipeline built on PDBFixer and RDKit. Structures
 200 were loaded from AlphaFold .pdb files. Nonstandard amino acid residues were identified and replaced
 201 with their standard equivalents to ensure consistency. All heterogens, including ligands, cofactors,
 202 and metal ions, were removed from the structure. Water molecules were also removed to reduce noise
 203 in the structural representation whilst missing hydrogen atoms were added at physiological pH (7.4).
 204 Finally, the cleaned and protonated structure was written to disk in PDB format and parsed into an
 205 RDKit molecule object for further processing [9].

206 **Docking protocol**

207 For each protein, we selected the binding site found by P2Rank with the highest probability. Then,
 208 using its coordinates, we built a cubic bounding region of 5 Å around the pocket using DeepChem.

209 Each box extends 5 Å in every direction from the center, resulting in a cube with 10 Å side length.
 210 The padding is automatically scaled based on the ligand’s dimensions to ensure the box is large
 211 enough to fully contain it, while still preserving the 5 Å margin around the ligand.

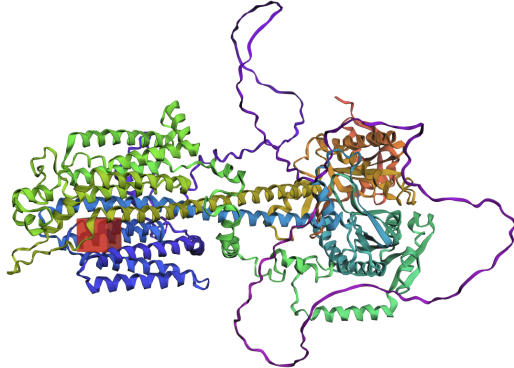


Figure 6: Binding pocket (in red) found by P2Rank on adcy5.

212 Lastly, we used AutoDock Vina through its Python extension to perform the docking, specifying
 213 5 poses per ligand and an exhaustiveness level of 8 [10]. We only kept the best score for each
 214 protein-ligand combination out of the 5 poses (i.e. the lowest score). The computations were executed
 215 on a High-Performance Computing (HPC) cluster, taking approximately 45 days to complete and
 216 600,000 CPU hours. We split the dataset into three folds by assigning all scores for certain proteins
 217 to separate subsets: 7 proteins for training, 1 for validation and 3 for testing. This setup provides
 218 a more realistic and challenging evaluation scenario, as models must generalize to unseen proteins
 219 rather than memorize patterns specific to a single target. It also avoids the overfitting risk of standard
 220 random splits, where the same protein might appear in both training and test sets.

221 Transformer architecture

222 To inform ML researchers and benchmark our dataset, we built a novel Transformer method to predict
 223 docking scores. We followed an embedding-based approach and used two foundation models to
 224 encode the protein and the ligand and perform the docking (Figure 7).

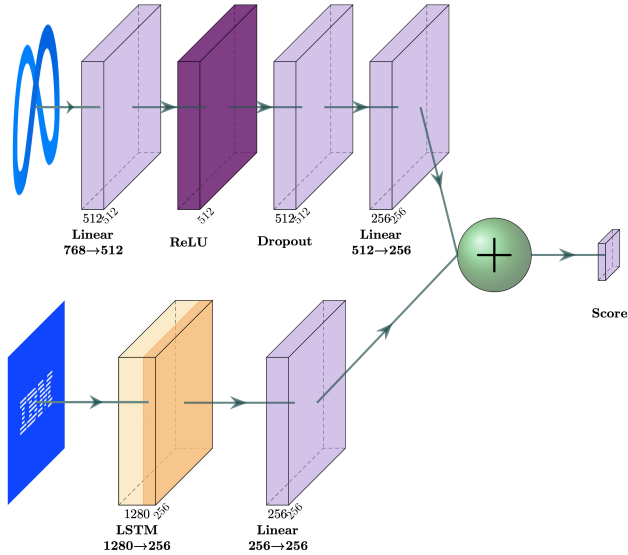


Figure 7: Architecture of the hybrid LSTM-FFN protein-ligand model.

225 The first model is ESM2, developed by Facebook AI Research (FAIR), which was pretrained on 250
226 million protein sequences comprising 86 billion amino acids [26]. Its learned representations capture
227 both local biochemical properties and long-range structural patterns, including secondary and tertiary
228 structures.

229 The second model is MolFormer, developed by IBM Research, which combines masked language
230 modeling with a linear attention Transformer and rotary positional embeddings [36]. It was pretrained
231 on 1.1 billion canonical SMILES strings from ZINC and PubChem. Canonicalization was performed
232 using RDKit to ensure consistency in representation. The model learns compact embeddings of
233 molecular structures and was fine-tuned on a range of downstream tasks.

234 We used both models to encode our set of 1.7 million molecules from ChEMBL and 16 proteins
235 from AlphaFold. The ESM2 model generates an embedding matrix $\mathbf{E} \in \mathbb{R}^{n \times 1280}$, where n is
236 the length of the protein sequence. Given the variability in protein sequence lengths, we pad all
237 embeddings to match the length of the longest protein, which is 1990, resulting in a final matrix
238 $\mathbf{E}_{\text{padded}} \in \mathbb{R}^{1990 \times 1280}$. The MolFormer model produces a fixed-size vector $\mathbf{V} \in \mathbb{R}^{768}$ for each
239 molecule. Formally, for a protein sequence P_i of length n_i and a molecule M , their embeddings are
240 represented as:

$$\mathbf{E}(P_i) = \begin{bmatrix} e_{1,1} & e_{1,2} & \cdots & e_{1,1280} \\ e_{2,1} & e_{2,2} & \cdots & e_{2,1280} \\ \vdots & \vdots & \ddots & \vdots \\ e_{n_i,1} & e_{n_i,2} & \cdots & e_{n_i,1280} \end{bmatrix} \in \mathbb{R}^{n_i \times 1280} \quad \text{and} \quad \mathbf{V}(M) = \begin{bmatrix} m_1 \\ m_2 \\ \vdots \\ m_{768} \end{bmatrix} \in \mathbb{R}^{768}$$

241 Final hybrid model

242 The docking model, implemented using PyTorch [33], is designed to predict the interaction between
243 ligands and proteins through a specialized architecture combining separate sub-models for ligands
244 and proteins. The ligand sub-model is a feedforward neural network, starting with an input dimension
245 of 768, matching the size of the MolFormer embedding. It includes two linear layers with a ReLU
246 activation and a dropout layer for regularization. The protein sub-model uses an LSTM (Long
247 Short-Term Memory) network to process sequential data, taking inputs with a dimension of 1280 to
248 match the size of the input embeddings from ESM2[18]. The output of the LSTM is further processed
249 through a linear layer to produce features that align in size with the ligand sub-model.

250 The model’s forward pass processes the ligand and protein embeddings through their respective
251 sub-models then concatenates these features into a combined vector. This vector is passed through a
252 regression layer that outputs the docking score prediction. The training phase involves calculating
253 the RMSE between predicted and actual scores and optimizing this loss using the Adam optimizer
254 [22] with a learning rate of 1×10^{-4} . We trained our models on an HPC cluster using a multi-GPU
255 setup with 8 Nvidia Tesla V100 (256 GB of VRAM in total). Each model was trained for 2 epochs
256 on the train set and used the validation set to print out the RMSE while training to look for signs of
257 overfitting.

258 Conclusion

259 We introduce Smiles2Dock, an open large-scale comprehensive dataset for training and benchmarking
260 ML-based protein-ligand docking algorithms from AlphaFold predicted structures. It uses well-
261 known chemical data sources such as AlphaFold and ChEMBL, a diverse set of biologically relevant
262 compounds on the same scale as modern molecular screening databases and is suitable for most major
263 approaches explore such as CNN, graph and embedding based methods. Moreover, existing datasets
264 rely on proteins with experimentally determined structures and known ligand binding pockets, making
265 them unusable for the growing number of proteins with only predicted structures. It is easy to use
266 for ML researchers and can be downloaded using two lines of code and a single library using the
267 Datasets library from HuggingFace. We also introduce a novel Transformer-based architecture that
268 uses ESM2 and Molformer to embed molecules and proteins in latent spaces and predict docking
269 scores.

270 **References**

271 [1] Tunde Aderinwale, Charles Christoffer, and Daisuke Kihara. Rl-mlzerd: Multimeric protein
272 docking using reinforcement learning. *Frontiers in Molecular Biosciences*, 9:969394, 2022.

273 [2] Vance W Berger and YanYan Zhou. Kolmogorov–smirnov test: Overview. *Wiley statsref:
274 Statistics reference online*, 2014.

275 [3] Bin Chong, Yingguang Yang, Zi-Le Wang, Han Xing, and Zhirong Liu. Reinforcement
276 learning to boost molecular docking upon protein conformational ensemble. *Physical Chemistry
277 Chemical Physics*, 23(11):6800–6806, 2021.

278 [4] Lee-Shin Chu, Jeffrey A Ruffolo, Ameya Harmalkar, and Jeffrey J Gray. Flexible protein–
279 protein docking with a multitrack iterative transformer. *Protein Science*, 33(2):e4862, 2024.

280 [5] Austin Clyde, Xuefeng Liu, Thomas Brettin, Hyunseung Yoo, Alexander Partin, Yadu Babuji,
281 Ben Blaiszik, Jamaludin Mohd-Yusof, Andre Merzky, Matteo Turilli, Shantenu Jha, Arvind
282 Ramanathan, and Rick Stevens. Ai-accelerated protein–ligand docking for sars-cov-2 is 100-fold
283 faster with no significant change in detection. *Scientific Reports*, 13:2105, February 2023.

284 [6] Ryan G. Coleman, Michael Carchia, Teague Sterling, John J. Irwin, and Brian K. Shoichet.
285 Ligand pose and orientational sampling in molecular docking. *PLoS ONE*, 8(10):e75992,
286 October 2013.

287 [7] Kevin Crampon, Alexis Giorkallos, Myrtille Deldossi, Stéphanie Baud, and Luiz Angelo
288 Steffenel. Machine-learning methods for ligand–protein molecular docking. *Drug Discovery
289 Today*, 27(1):151–164, January 2022.

290 [8] Christopher DeBoever, Yosuke Tanigawa, Malene E Lindholm, Greg McInnes, Adam Lavertu,
291 Erik Ingelsson, Chris Chang, Euan A Ashley, Carlos D Bustamante, Mark J Daly, et al. Medical
292 relevance of protein-truncating variants across 337,205 individuals in the uk biobank study.
293 *Nature communications*, 9(1):1612, 2018.

294 [9] Peter Eastman, Jason Swails, John D Chodera, Robert T McGibbon, Yutong Zhao, Kyle A
295 Beauchamp, Lee-Ping Wang, Andrew C Simmonett, Matthew P Harrigan, Chaya D Stern, et al.
296 Openmm 7: Rapid development of high performance algorithms for molecular dynamics. *PLoS
297 computational biology*, 13(7):e1005659, 2017.

298 [10] Jerome Eberhardt, Diogo Santos-Martins, Andreas F. Tillack, and Stefano Forli. Autodock vina
299 1.2.0: New docking methods, expanded force field, and python bindings. *Journal of Chemical
300 Information and Modeling*, 61(8):3891–3898, July 2021.

301 [11] Richard A Friesner, Jay L Banks, Robert B Murphy, Thomas A Halgren, Jasna J Klicic, Daniel T
302 Mainz, Matthew P Repasky, Eric H Knoll, Mee Shelley, Jason K Perry, et al. Glide: a new
303 approach for rapid, accurate docking and scoring. 1. method and assessment of docking accuracy.
304 *Journal of medicinal chemistry*, 47(7):1739–1749, 2004.

305 [12] Miguel García-Ortegón, Gregor N. C. Simm, Austin J. Tripp, José Miguel Hernández-Lobato,
306 Andreas Bender, and Sergio Bacallado. Dockstring: Easy molecular docking yields better bench-
307 marks for ligand design. *Journal of Chemical Information and Modeling*, 62(15):3486–3502,
308 July 2022.

309 [13] Anna Gaulton, Louisa J Bellis, A Patricia Bento, Jon Chambers, Mark Davies, Anne Hersey,
310 Yvonne Light, Shaun McGlinchey, David Michalovich, Bissan Al-Lazikani, et al. Chemb: a
311 large-scale bioactivity database for drug discovery. *Nucleic acids research*, 40(D1):D1100–
312 D1107, 2012.

313 [14] Daniel A Gschwend, Andrew C Good, and Irwin D Kuntz. Molecular docking towards drug
314 discovery. *Journal of Molecular Recognition: An Interdisciplinary Journal*, 9(2):175–186,
315 1996.

316 [15] Linyuan Guo, Tian Qiu, and Jianxin Wang. Vitscore: a novel three-dimensional vision trans-
317 former method for accurate prediction of protein–ligand docking poses. *IEEE transactions on
318 nanobioscience*, 2023.

319 [16] Linyuan Guo and Jianxin Wang. Vitrmse: a three-dimensional rmse scoring method for protein-
320 ligand docking models based on vision transformer. In *2022 IEEE International Conference on*
321 *Bioinformatics and Biomedicine (BIBM)*, pages 328–333. IEEE, 2022.

322 [17] Ye Han, Fei He, Yongbing Chen, Wenyuan Qin, Helong Yu, and Dong Xu. Quality assessment of
323 protein docking models based on graph neural network. *Frontiers in Bioinformatics*, 1:693211,
324 2021.

325 [18] Sepp Hochreiter and Jürgen Schmidhuber. Long short-term memory. *Neural computation*,
326 9(8):1735–1780, 1997.

327 [19] Huaipan Jiang, Mengran Fan, Jian Wang, Anup Sarma, Shruti Mohanty, Nikolay V Dokholyan,
328 Mehrdad Mahdavi, and Mahmut T Kandemir. Guiding conventional protein–ligand docking
329 software with convolutional neural networks. *Journal of chemical information and modeling*,
330 60(10):4594–4602, 2020.

331 [20] Huaipan Jiang, Jian Wang, Weilin Cong, Yihe Huang, Morteza Ramezani, Anup Sarma, Niko-
332 lay V. Dokholyan, Mehrdad Mahdavi, and Mahmut T. Kandemir. Predicting protein–ligand
333 docking structure with graph neural network. *Journal of Chemical Information and Modeling*,
334 62(12):2923–2932, June 2022.

335 [21] John Jumper, Richard Evans, Alexander Pritzel, Tim Green, Michael Figurnov, Olaf Ron-
336 neberger, Kathryn Tunyasuvunakool, Russ Bates, Augustin, Anna Potapenko, et al. Highly
337 accurate protein structure prediction with alphafold. *Nature*, 596(7873):583–589, 2021.

338 [22] Diederik P Kingma and Jimmy Ba. Adam: A method for stochastic optimization. *arXiv preprint*
339 *arXiv:1412.6980*, 2014.

340 [23] Thomas Kluyver, Benjamin Ragan-Kelley, Fernando Pérez, Brian E Granger, Matthias Bus-
341 sonnier, Jonathan Frederic, Kyle Kelley, Jessica B Hamrick, Jason Grout, Sylvain Corlay,
342 et al. Jupyter notebooks-a publishing format for reproducible computational workflows. *Elpub*,
343 2016:87–90, 2016.

344 [24] Radoslav Krivák and David Hokszá. P2rank: machine learning based tool for rapid and accurate
345 prediction of ligand binding sites from protein structure. *Journal of Cheminformatics*, 10(1),
346 August 2018.

347 [25] Quentin Lhoest, Albert Villanova del Moral, Yacine Jernite, Abhishek Thakur, Patrick von
348 Platen, Suraj Patil, Julien Chaumont, Mariama Drame, Julien Plu, Lewis Tunstall, et al. Datasets:
349 A community library for natural language processing. *arXiv preprint arXiv:2109.02846*, 2021.

350 [26] Zeming Lin, Halil Akin, Roshan Rao, Brian Hie, Zhongkai Zhu, Wenting Lu, Nikita Smetanin,
351 Robert Verkuil, Ori Kabeli, Yaniv Shmueli, Allan dos Santos Costa, Maryam Fazel-Zarandi,
352 Tom Sercu, Salvatore Candido, and Alexander Rives. Evolutionary-scale prediction of atomic
353 level protein structure with a language model, July 2022.

354 [27] Andreas Luttens, Israel Cabeza de Vaca, Leonard Sparring, Ulf Norinder, and Jens Carlsson.
355 Rapid traversal of ultralarge chemical space using machine learning guided docking screens,
356 May 2023.

357 [28] John I Marden. Positions and qq plots. *Statistical Science*, pages 606–614, 2004.

358 [29] Andrew T McNutt, Paul Francoeur, Rishal Aggarwal, Tomohide Masuda, Rocco Meli, Matthew
359 Ragoza, Jocelyn Sunseri, and David Ryan Koes. Gnina 1.0: molecular docking with deep
360 learning. *Journal of cheminformatics*, 13(1):43, 2021.

361 [30] Xuan-Yu Meng, Hong-Xing Zhang, Mihaly Mezei, and Meng Cui. Molecular docking: a
362 powerful approach for structure-based drug discovery. *Current computer-aided drug design*,
363 7(2):146–157, 2011.

364 [31] Garrett M Morris and Marguerita Lim-Wilby. Molecular docking. *Molecular modeling of*
365 *proteins*, pages 365–382, 2008.

366 [32] Marina A Pak, Karina A Markhieva, Mariia S Novikova, Dmitry S Petrov, Ilya S Vorobyev,
367 Ekaterina S Maksimova, Fyodor A Kondrashov, and Dmitry N Ivankov. Using alphafold to pre-
368 dict the impact of single mutations on protein stability and function. *Plos one*, 18(3):e0282689,
369 2023.

370 [33] Adam Paszke, Sam Gross, Francisco Massa, Adam Lerer, James Bradbury, Gregory Chanan,
371 Trevor Killeen, Zeming Lin, Natalia Gimelshein, Luca Antiga, Alban Desmaison, Andreas
372 Köpf, Edward Yang, Zach DeVito, Martin Raison, Alykhan Tejani, Sasank Chilamkurthy,
373 Benoit Steiner, Lu Fang, Junjie Bai, and Soumith Chintala. Pytorch: An imperative style,
374 high-performance deep learning library, 2019.

375 [34] Robert M Plenge, Edward M Scolnick, and David Altshuler. Validating therapeutic targets
376 through human genetics. *Nature reviews Drug discovery*, 12(8):581–594, 2013.

377 [35] Nornadiah Mohd Razali, Yap Bee Wah, et al. Power comparisons of shapiro-wilk, kolmogorov-
378 smirnov, lilliefors and anderson-darling tests. *Journal of statistical modeling and analytics*,
379 2(1):21–33, 2011.

380 [36] Jerret Ross, Brian Belgodere, Vijil Chenthamarakshan, Inkil Padhi, Youssef Mroueh, and Payel
381 Das. Large-scale chemical language representations capture molecular structure and properties.
382 *Nature Machine Intelligence*, 4(12):1256–1264, December 2022.

383 [37] Saori Sakaue, Masahiro Kanai, Yosuke Tanigawa, Juha Karjalainen, Mitja Kurki, Seizo Koshiba,
384 Akira Narita, Takahiro Konuma, Kenichi Yamamoto, Masato Akiyama, et al. A cross-population
385 atlas of genetic associations for 220 human phenotypes. *Nature genetics*, 53(10):1415–1424,
386 2021.

387 [38] Francesca Stanzione, Ilenia Giangreco, and Jason C. Cole. *Use of molecular docking computa-*
388 *tional tools in drug discovery*, page 273–343. Elsevier, 2021.

389 [39] Yosuke Tanigawa, Jiehan Li, Johanne M Justesen, Heiko Horn, Matthew Aguirre, Christopher
390 DeBoever, Chris Chang, Balasubramanian Narasimhan, Kasper Lage, Trevor Hastie, et al.
391 Components of genetic associations across 2,138 phenotypes in the uk biobank highlight
392 adipocyte biology. *Nature communications*, 10(1):4064, 2019.

393 [40] Yosuke Tanigawa, Michael Wainberg, Juha Karjalainen, Tuomo Kiiskinen, Guhan Venkatara-
394 man, Susanna Lemmelä, Joni A Turunen, Robert R Graham, Aki S Havulinna, Markus Perola,
395 et al. Rare protein-altering variants in angrl7 lower intraocular pressure and protect against
396 glaucoma. *PLoS Genetics*, 16(5):e1008682, 2020.

397 [41] Wen Torng and Russ B Altman. Graph convolutional neural networks for predicting drug-target
398 interactions. *Journal of chemical information and modeling*, 59(10):4131–4149, 2019.

399 [42] Viet-Khoa Tran-Nguyen, Célien Jacquemard, and Didier Rognan. Lit-pcba: an unbiased data
400 set for machine learning and virtual screening. *Journal of chemical information and modeling*,
401 60(9):4263–4273, 2020.

402 [43] Oleg Trott and Arthur J. Olson. Autodock vina: Improving the speed and accuracy of docking
403 with a new scoring function, efficient optimization, and multithreading. *Journal of Computa-*
404 *tional Chemistry*, 31(2):455–461, June 2009.

405 [44] Xiao Wang, Sean T Flannery, and Daisuke Kihara. Protein docking model evaluation by graph
406 neural networks. *Frontiers in Molecular Biosciences*, 8:647915, 2021.

407 [45] Clark Wissler. The spearman correlation formula. *Science*, 22(558):309–311, 1905.

408 [46] Liangzhen Zheng, Jingrong Fan, and Yuguang Mu. Onionnet: a multiple-layer intermolecular-
409 contact-based convolutional neural network for protein–ligand binding affinity prediction. *ACS*
410 *omega*, 4(14):15956–15965, 2019.